LES OF TRANSITIONAL BOUNDARY LAYER AT HIGH FREE-STREAM TURBULENCE INTENSITY, AND IMPLICATIONS FOR RANS MODELLING

Sylvain Lardeau
Ning Li
Michael A. Leschziner
Imperial College London, Department of Aeronautics
Prince Consort Road, South Kensington
London, UK, SW7 2AZ

ABSTRACT

Large-eddy simulations of a transitional flow over a flat plate are performed for different free-stream conditions. Interest focuses, in particular, on the mechanisms in the boundary layer before transition occurs, the practical context being flow over turbine blades. These considerations are motivated by the wish to study the realism of a RANS-type model designed to return the "laminar fluctuation energy" observed well upstream of the location at which transition sets in. The assumptions underlying the model are discussed in the light of turbulence-energy budgets deduced from the simulations. It is shown that the pre-transitional field is characterised by elongated streaky structures which, notwithstanding the very different structural properties, lead to the amplification of fluctuations by conventional shear-stress / strain interaction, rather than by pressure diffusion, the latter being the process central to the formulation of the RANS-type model.

INTRODUCTION

Bypass transition from the laminar to the turbulent state occurs when the linear growth of Tollmien-Schlichting waves, preceding natural transition, is bypassed by the penetration of disturbances into the boundary layer from a highly turbulent free stream. This process is especially pertinent to the flow over turbine blades. In low-pressure cascades, in particular, the Reynolds number, based on blade chord, is of the order 10^5. This relatively low value, in combination with the acceleration of the flow in the cascade passages, can result in the boundary layer of the blade being laminar or transitional over 50-70% of the blade surface. In such circumstances, the transition process can have major operational consequences. In particular, early transition may prevent separation (stall) of the suction-side boundary layer, which is subjected, towards the rear of the blade, to a locally adverse pressure gradient. The consequence is a significant reduction in total-pressure loss. Furthermore, bypass transition plays an important role in the response of the suction-side boundary layer to passing wakes of preceding blade stages (Fig. 1).

Turbomachine flows are almost invariably modelled within the RANS framework with statistical closures that are applicable to fully-established turbulence, and the representation of bypass transition within this framework presents a major challenge. Virtually all approaches return the transition process, in one way or another, as a rapid rise in turbulence activity at a specific transition location along the blade boundary layer, with consequent rapid rise in skin friction and heat-transfer coefficient. Transition is variously modelled with correlations for an intermittency parameter, with intermittency-transport equations or with low-Reynolds-number turbulence-transport equations, which induce transition when the free-stream turbulence diffusing into the boundary layer is amplified by production to the extent of exceeding viscous dissipation. Reality is much more intricate, however.

Both experiments and simulations show that the boundary layer contains a significant level of "turbulence" well before the skin friction rises - the latter conventionally identifying transition. However, this "turbulence" does not comply with the usual concept of the condition in which the turbulence energy and the shear stress (and hence skin friction) are closely correlated. What is observed, rather, is that the fluctuation intensity rises in the intermediate-to-upper reaches of the boundary layer, well ahead of the rise in shear stress, giving a ratio of $\langle uv \rangle / k$ far below that associated with established turbulence. Turbulence models, either with or without transition corrections, are not able to return this "pre-transitional" behaviour (Lardeau et al., 2004b).

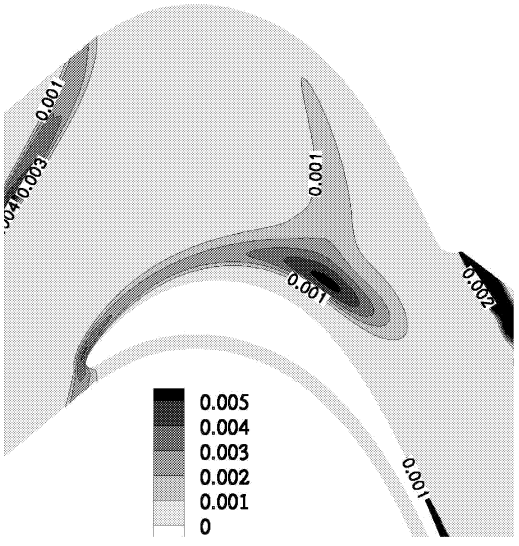

Figure 1: Turbulence energy in blade passage, wake created by a moving rod, T106A blade profile.

Observing that the pre-transitional velocity profile essentially adhered to laminar criteria, Mayle and Schulz (1997) proposed an equation for the *laminar kinetic energy*, formally

similar to the conventional form governing the turbulence energy, to represent the pre-transitional rise in fluctuation level. This equation lacks the usual shear-stress/strain-related generation term, but contains a source term that is argued to arise from the pressure-diffusion correlation. Thus, the equation returns, upon calibration, the requisite rise in the fluctuation-energy level in the laminar regime, despite the absence of a shear stress, which is presumed to be zero. Mayle and Schulz's equation was used by Lardeau and Leschziner (2004b,2005) to construct a transition-modified low-Reynolds-number, nonlinear eddy-viscosity model capable of returning the correct behaviour of transitional as well as pre-transitional features in laboratory configurations of the type shown in Fig. 1, in which passing wakes generated by moving cylinders provoke, in conjunction with high free-stream turbulence, unsteady transition. However, an open question that was not addressed was whether the pre-transitional model for the *laminar kinetic energy* is conceptually correct. To answer this question, highly-resolved large eddy simulations have been performed of a boundary layer developing over a flat plate, subjected to free-stream turbulence. In particular, the influence of the turbulence structure in the free stream was examined, and turbulence budgets were obtained to study implications when modelling the process within a statistical framework, and to examine the validity of Mayle and Schulz's (1997) proposal. It is this study that is reported herein.

Several earlier simulations and experimental investigations, dealing with various aspects of bypass transition, have already been published. These consider, among other issues, the influence of free-stream-turbulence intensity, the properties of the spectra of this turbulence and the effects of pressure gradient (e.g. Matsubara and Alfredsson, 2001, Jacobs and Durbin, 2001, Brandt et al., 2004). The study by Brandt et al. (2004), in particular, shows that the details of the transition process are sensitive to the integral length scale in the free stream, and that receptivity of long streaky structures in the boundary layer to free-stream turbulence depends on the spectral distribution of modes in that stream. To the present authors' knowledge, only one study, namely that by Voke and Yang (1995), includes considerations on how the budgets of the Reynolds stresses evolve before and during transition. However, these simulations have been done with low numerical accuracy, and several processes of the budget have been agglomerated into groups, not allowing some important processes to be distinguished in isolation from others. The present study addresses, among other issues, the evolution of the budgets, with particular attention focusing on shear production relative to pressure-velocity interaction.

THE COMPUTATIONAL FRAMEWORK

The simulations were performed with a staggered finite-difference scheme, combining a second-order Adams-Bashforth scheme for the time integration with a second-order central-difference scheme for the spatial derivatives. Subgrid-scale processes are represented by the Localized Lagrangian-averaged dynamic eddy-viscosity model, proposed by Meneveau et al. (1996). This has been reported by Sarghini et al. (1999) to perform especially well in transitional flows, and is thus held to be well suited to the present study.

The domain size and grid resolution are, respectively $(L_x, L_y, L_z) = (400\delta_1^*, 35\delta_1^*, 40\delta_1^*)$, where δ_1^* is the displacement thickness at the inlet, and $(n_x, n_y, n_z) = (512, 80, 96)$ points. The momentum-thickness Reynolds number, based on the inflow condition, is equal to 425 for all the simulations. Statistical data, including budgets, have been obtained by integrating over a period equal to $2650\delta_1^*/U_{in}$ and the homogeneous spanwise direction.

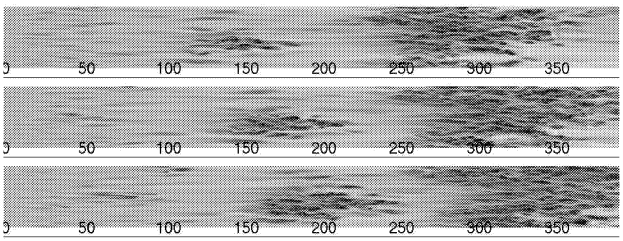

Figure 2: Contours of the streamwise component of the velocity in the (x, z) plane, simulation S_{iso}

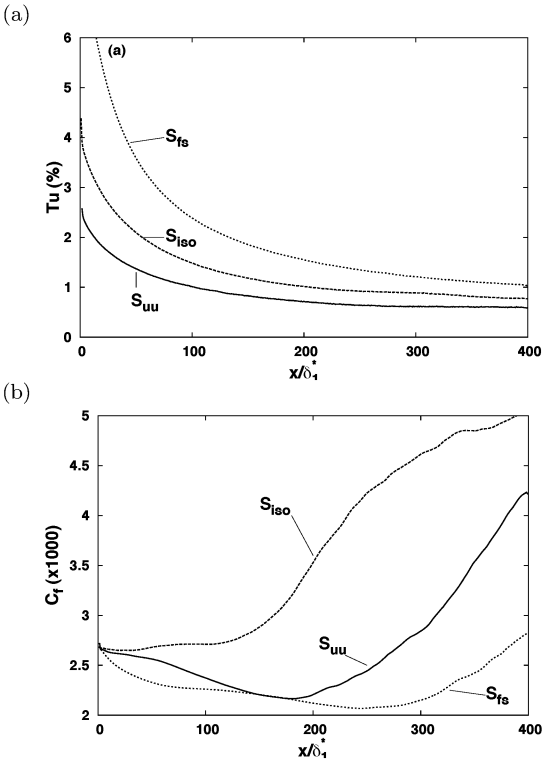

Figure 3: Streamwise evolution of (a) the free-stream turbulence intensity and (b) the skin-friction coefficient.

The free-stream turbulence at the inlet was synthetically generated by a Fourier-series method (Rogallo, 1981), which satisfies a prescribed spectrum, given by

$$E(k) = \frac{2}{3}\frac{a(k/k_p)^4}{(b + (k/k_p)^2)^{17/6}} \qquad (1)$$

where $a = 1.606$ and $b = 1.350$, k is the wavenumber and k_p is peak wavenumber. This method preserves spatial and temporal coherence and includes random sampling in respect of the phase of the Fourier components (Lardeau et al., 2004a). An alternative method, proposed by Jacobs and Durbin (2001) and used by Brandt et al. (2004), is to superimpose onto the

free-stream spectrum the modes of the continuous spectrum of the linearised Orr-Sommerfeld and Squire operators. This method is appropriate if the goal is to study the detailed spectral mechanisms and receptivity issues over the full domain, including the stability region, where the small-amplitude perturbations are important. In contrast, the principal aim of the present study is to examine the statistical properties of the pre-transitional and the initial stages of the transitional region for different free-stream conditions. To this end, a refined spectral treatment of the free stream is not needed.

Three simulations are discussed below. In one, denoted $S_{\rm iso}$, isotropic turbulence is prescribed in the free-stream and at the inlet plane, including within the boundary layer which is prescribed at the inlet. In the second, identified as S_{fs}, isotropic turbulence is prescribed, but only above the blasius boundary layer. Finally, in the third, denoted S_{uu}, only streamwise fluctuations are prescribed. The aim of the last is to re-examine more carefully Voke and Yang's observation (1995) that low lateral fluctuations in the free tream inhibit transition, due to the weakness of pressure fluctuations induced by these later fluctuations. The results of such simulations appear not to have been published. As will be shown below, the absence of perturbations prescribed in the boundary layer at the inlet (case S_{fs}) lacks the elongated streaky structures observed in the two other simulations, which are the receptivity sites for free-stream turbulence and which eventually break down into turbulent spots (Brandt et al., 2004). As a consequence, transition is delayed beyond the end of the computational domain if the value of Tu used in S_{iso} is maintained for S_{fs}. Thus, for this case, the free-stream turbulence intensity at inlet was raised to 8%. This is a permissible practice in view of the fact that the objective is to examine the evolution of the statistical properties around and upstream of the transition onset. Finally, the inlet level of Tu in the simulation S_{uu} is lower than in S_{iso}, arising from the fact that the level of $\langle uu \rangle$ has been kept the same in both simulations, while the other two components have been nullified in S_{uu}.

RESULTS

An overall impression of the transition process is conveyed in Fig. 2, which shows contours of the streamwise fluctuations derived from the simulation S_{iso} at three time levels separated by the interval $45\delta_1^*/U_{in}$. These images are very similar to those observed experimentally by Matsubara and Alfredsson (2001) and numerically by Brandt et al. (2004). Thus, elongated structures are visible right from the inlet, and these structures eventually breakdown into turbulent spots at around $x = 110\delta_1^*$. As will be shown below, this is also roughly the location at which the skin friction rises. It is observed that the streaks are also present downstream of the spots. Even further downstream, the turbulent spots merge into a fully turbulent flow.

Fig. 3 shows the streamwise decay of the free-stream turbulence intensity and the corresponding evolution of the skin friction. The transition process is clearly a strong function of the turbulence structure in the free stream and in the boundary layer. Conventionally, transition is considered to set in when the skin friction rises significantly. This occurs at around x/δ_1^* =130, 180 and 300 for S_{iso}, S_{uu} and S_{fs}, respectively, the first value being close to that at which the turbulent spots first develop in Fig. 2. In every cases, the skin friction indicates a slow transition process. This is especially so with

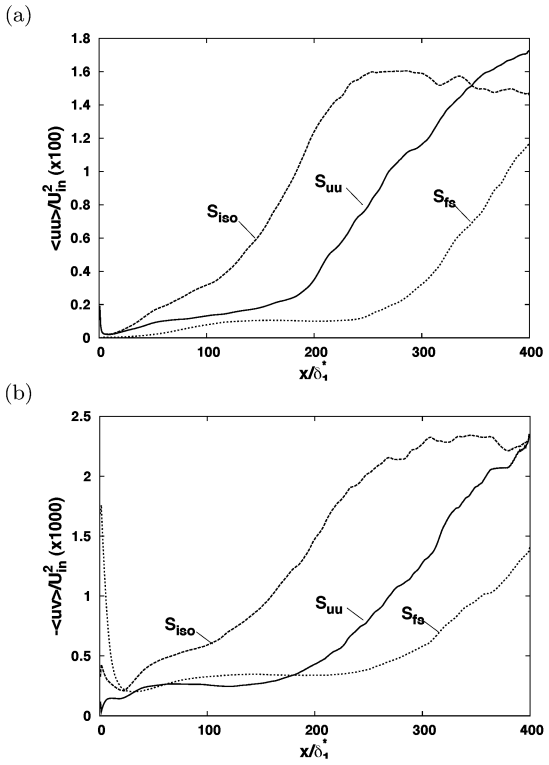

Figure 4: (a) Streamwise evolution of the streamwise velocity fluctuations close to the wall ($y/\delta_1^* = 0.34$) (b) streamwise evolution of the shear stress.

S_{fs}, despite the much higher free-stream-turbulence intensity that is applied in the other two cases. With no perturbations in the boundary layer, Brandt et al. (2004) argue that "shear sheltering" prevents the free-stream fluctuations from entering the boundary layer. In the other two simulations, the perturbations introduced inside the boundary layer create long streamwise structures (Fig. 2), which are receptivity sites for the fluctuations entering the boundary layer. What may also be concluded from Fig. 3 is that the suppression of lateral free-stream fluctuations (i.e. a high level of anisotropy) does indeed inhibit the transition process.

Fig. 4 shows the streamwise evolution of $\langle uu \rangle$ and $\langle uv \rangle$ at a distance $y = 0.34\delta_1^*$ from the wall. Although the imposed perturbation fields differ substantially, the evolutions of $\langle uu \rangle$ are qualitatively similar. As observed experimentally by Matsubara and Alfreddson (2001), the energy is proportional to the distance from the leading edge. In the case S_{iso}, to which Fig. 2 relates, the streamwise-normal and shear stresses are seen to rise well upstream of the location at which C_f begins to increase. This rise is due to the long streaks that develop well upstream of the transition, while the turbulent spots are responsible for the elevation of the C_f value. The simulation S_{fs} shows an especially interesting behaviour. Initially, the boundary layer is laminar and features no streaks, so the value of $\langle uu \rangle$ is very low. It then increases almost linearly between the inlet and $x = 100\delta_1^*$, the level remaining low, because of low receptivity, until the onset of transition, at around $x = 300\delta_1^*$.

Fig. 5 gives streamwise distributions of the ratio $-\langle uv \rangle/k$ at four wall-normal locations. In this connection, it will be

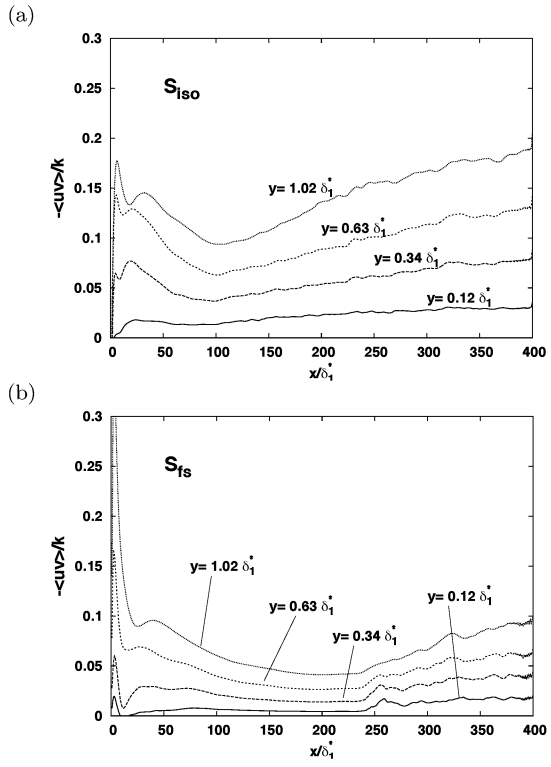

Figure 5: Streamwise evolution of the ratio $-\langle uv\rangle/k$ at different distance from the wall, simulation (a) S_{iso} and (b) S_{fs} .

recalled that the Mayle and Schulz model rests on the assumption of zero shear stress and zero shear-strain generation. As seen from the distributions relating to S_{iso}, this notion is incorrect. Clearly, the ratio is fairly high - of order 30%-50% of the level in a fully turbulent boundary layer - signifying an elevated shear stress upstream of transition. While the ratio $-\langle uv\rangle/k$ declines sharply as the wall is approached, there is no fundamental or sudden change in this ratio as the flow undergoes transition at around $x = 130\delta_1^*$, except for the distinctive rise in the boundary-layer portion remote from the wall. When turbulence is suppressed in the inlet boundary layer, as done in S_{fs}, so that receptivity is drastically reduced, the ratio is much lower, and this is consistent with the substantially delayed transition observed in Fig. 3.

Budgets for the turbulence energy are given in Figs. 6 to 8. The various curves correspond to the terms identified in equation 2 below:

$$\underbrace{U_j\frac{\partial k}{\partial x_j}}_{\text{Conv}} = \underbrace{-\langle u_i u_j\rangle\frac{\partial U_i}{\partial x_j}}_{P_k} \underbrace{-\frac{\partial\langle k' u_j\rangle}{\partial x_j}}_{D_t} \underbrace{-\frac{1}{\rho}\frac{\partial\langle p u_j\rangle}{\partial x_j}}_{D_p} + \underbrace{\nu\frac{\partial^2 k}{\partial x_i\partial x_i}}_{D_\nu} - \varepsilon \quad (2)$$

These represent, respectively, convection, production, turbulent diffusion, pressure diffusion, viscous diffusion and dissipation. The budgets are plotted at different streamwise locations, but in all cases before transition sets in, as identified by the skin-friction rise in Fig. 3. Also plotted, by way of square symbols, is the production term proposed by Mayle and Schulz (1997) in their pre-transition laminar-fluctuation

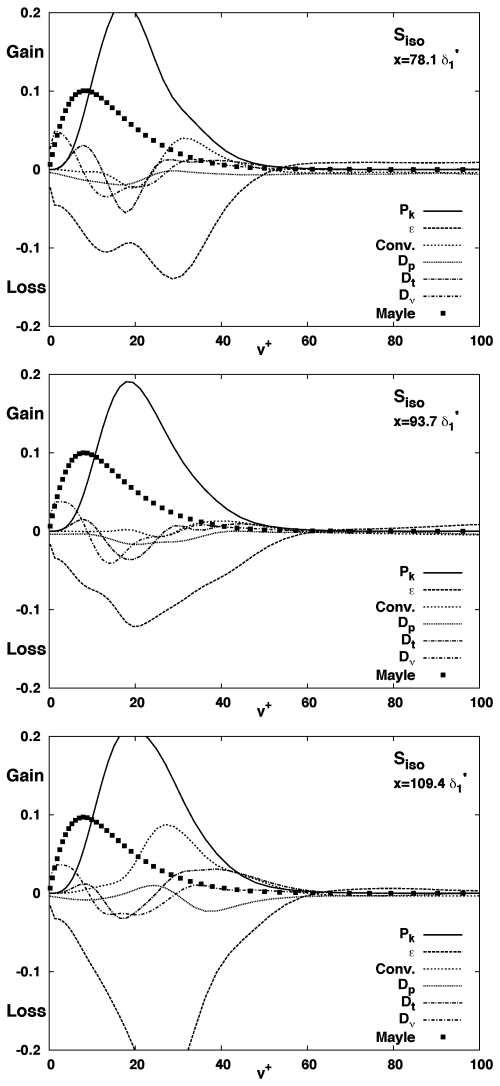

Figure 6: Turbulence-energy budgets (equation (2)) for the S_{iso} test case.

model:

$$P_{k_l} = C_\omega \frac{U_{in}^2}{\nu}\sqrt{k.k_\infty}\exp -y^+/C^+ \quad (3)$$

In contrast to the presentation adopted by Voke and Yang (1995), the different processes featuring in equation (2) have here been separated. Attention is drawn to the fact that the dissipation rate ε in the budgets is that resolved by the simulation. However, this level (ε_{res}) is more than 95% of the total (with the subgrid-scale contribution estimated from the subgrid-scale model), illustrating the quality of the resolution and the relatively modest contribution of the unresolved processes.

As noted earlier, Mayle and Schulz's model is based on the hypothesis that shear-induced production is zero, while the amplification of pre-transitional fluctuation energy is effected by way of the pressure diffusion. As seen from Fig. 6, relating to S_{iso}, the simulation provides no evidence that this scenario is realistic. Thus, the elevation of fluctuation energy is due to shear production, despite the relatively low level of the shear

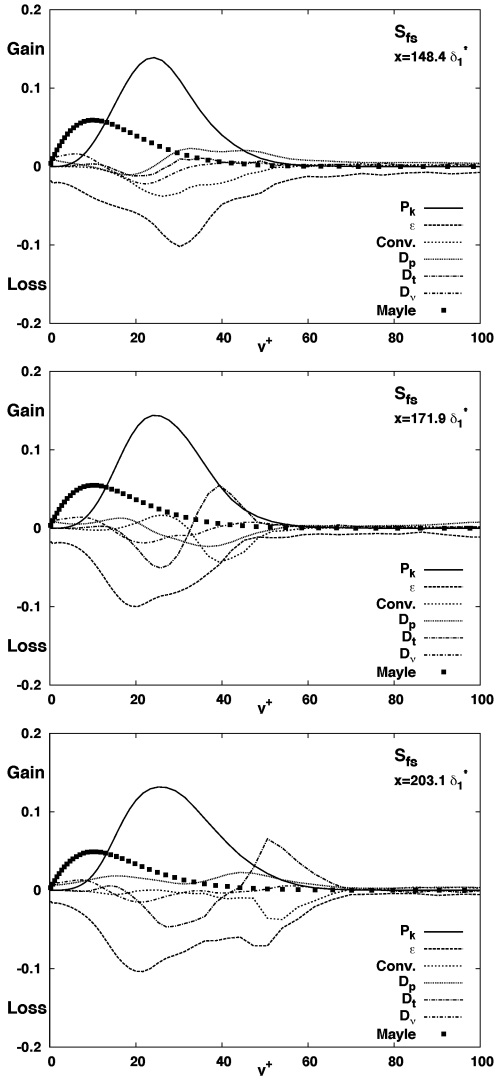

Figure 7: Turbulence-energy budgets (equation (2)) for the S_{fs} test case.

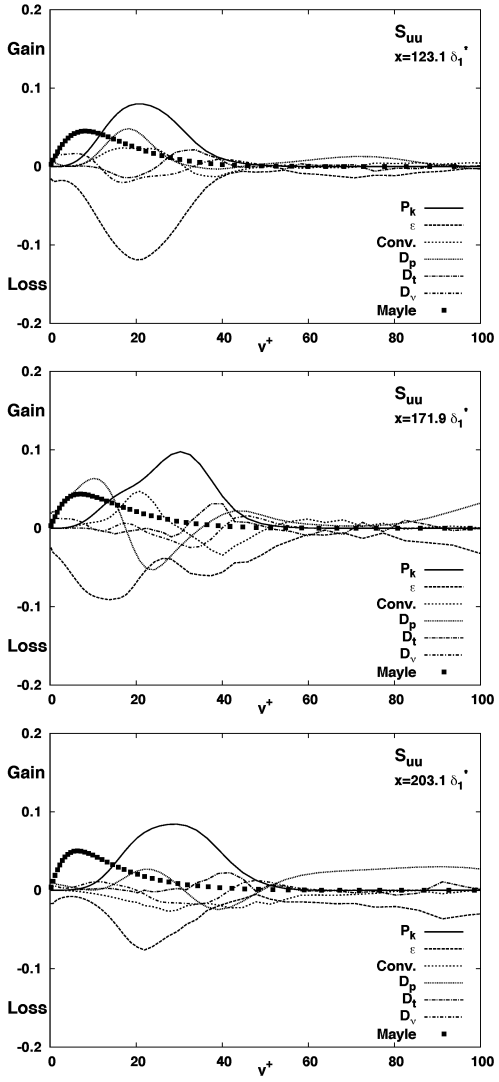

Figure 8: Turbulence-energy budgets (equation (2)) for the S_{uu} test case.

stress. In contrast, pressure diffusion is minor - indeed, negative - over most of the boundary layer. While the balance is predominantly between production and dissipation, the budget clearly differs substantially from that of a fully turbulent layer. In particular, dissipation declines towards the wall due to the low level of diffusion. Thus, close to the wall, turbulence activity is insignificant.

The budgets derived from simulations S_{fs} and S_{uu} are qualitatively similar to that discussed above. A surprising observation, at first sight, is that the latter is characterised by significantly lower levels of production and hence also dissipation relative to those of the other two simulations. A partial explanation can be derived from Fig. 4. This shows the shear stress to be especially low in simulation S_{uu}, while the level of $\langle uu \rangle$ (and hence k) is higher than that of simulation S_{fs}. Thus, the $\langle uv \rangle$-related production is especially low in the pre-transitional region, despite the presence of the elongated streaks is S_{uu}. This suggests that receptivity associated with the streaky structure upstream of the spots is not the only feature that governs transition, but that highly anisotropic free-stream fluctuations also play an important role - as has already been concluded by reference to Fig. 4. Despite these differences, the principal message is that in all three simulations the balance is mainly between shear production and dissipation, while pressure diffusion is negligible, except in some parts of the boundary layer of simulation S_{uu}, where it does seem to act in the same sense as the production term. Mayle and Schulz's model is seen to return a behaviour which is bound to increase the pre-transitional fluctuation energy, but the level is too low, and the maximum much too close to the wall.

Finally, plotted on Fig. 9 are anisotropy maps which correlate the third and second anisotropy invariants across the flow at the same streamwise positions for which the budgets have been reported. The trajectories on the (**III**,-**II**) plane show that, before transition, the flow tends towards the one-component limit in the near-wall region, especially for the S_{uu} case for which the free stream is itself close to the

one-component state. For the two cases, in which isotropic turbulence is prescribed in the free stream, there is a progressive departure from isotropy towards the one component state. An interesting feature is that, in the case S_{uu}, the conditions in the middle portion of the boundary layer first show a trend towards isotropy, with subsequent approach to the one-component limit.

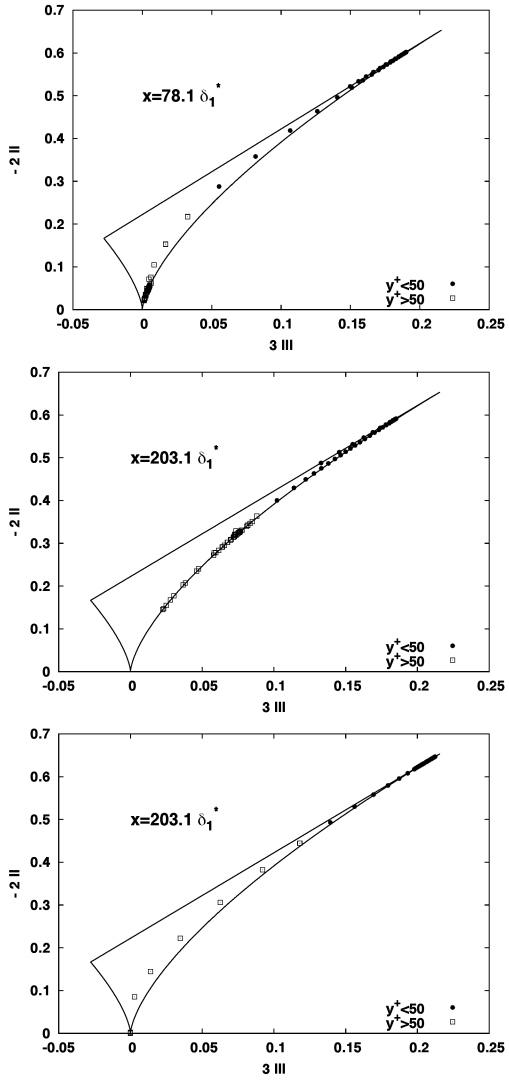

Figure 9: Anisotropy-invariants map for (from top to bottom) S_{iso}, S_{uu} and S_{fs} test cases.

CONCLUSIONS

Although the simulations are subject of some uncertainties arising from the lack of realism in the free-stream conditions, relative to those in a typical experiment, the results are relevant and informative. In particular, the principal objective of shedding light on the validity of the basic assumptions underlying a closure for the high fluctuation level observed upstream of the transition location has been met. The simulations show that, from a statistical point of view, shear-stress/shear-strain-induced production is mainly responsible for the elevation of the pre-transitional "laminar fluctuation energy" - a process that is akin to that observed in the turbulent state, although effective here mainly in the upper (wall-remote) portions of the boundary layer. Indeed, the ratio $\langle uv \rangle / k$ is fairly high over a significant portion of the pre-transitional boundary layer away from the wall, relative to the value 0.3 associated with an equilibrium boundary layer. This contradicts the basis of the model investigated herein, which rests on the assumption that the shear stress and the shear production is zero. The simulations also show that a highly anisotropic state in the free stream, wherein lateral fluctuations are very low, or the absence of fluctuations in the laminar boundary layer subjected to isotropic free-stream turbulence leads to a significant reduction in receptivity and a substantial delay in the formation of turbulent spots, which mark the onset of transition. The expectation is that lessons and data derived from this study will result in an improved model for the pre-transitional processes.

ACKNOWLEDGEMENTS

The research reported herein was undertaken within the project 'Unsteady Transitional Flows in Axial Turbomachinery', funded by the European Commission under contract G4RD-CT-2001-00628.

REFERENCES

Brandt, L., Schlatter, P., and Henningson, D. (2004). Transition in boundary layers subject to free-stream turbulence. *J. Fluid Mech.*, **517**:167-198.

Jacobs, R. and Durbin, P. (2001). Simulations of bypass transition. *J. Fluid Mech.*, **428**:185–212.

Lardeau, S., Lamballais, E., and Bonnet, J. (2004a). Effect of velocity ratio on the spatial development of a plane mixing layer. *Phys. Fluids*, in preparation.

Lardeau, S., Leschziner, M., and Li, N. (2004b). Modelling bypass transition with low-reynolds-number non-linear eddy-viscosity closure. *Flow, Turbulence and Combustion*, **73**: 49-76

Lardeau, S., and Leschziner, M. (2005). Unsteady RANS modelling of wake-induced transition in linear LP-turbine cascades. *AIAA J.*, submitted.

Matsubara, M. and Alfredsson, P.H. (2001). Disturbance growth in boundary layers subjected to free-stream turbulence. *J. Fluid Mech.*, **430**:149–168.

Mayle, R. and Schulz, A. (1997). The path to predicting bypass transition. *J. of Turbomachinery*, **119**:405–411.

Meneveau, C., Lund, T., and Cabot, W. (1996). A lagrangian dynamic subgrid-scale model of turbulence. *J. Fluid Mech.*, **319**:353–385.

Rogallo, R. (1981). Numerical experiments in homogeneous turbulence. Tech. Memo. 81315, NASA.

Sarghini, F., Piomelli, U., and Balaras, E. (1999). Scale-similar models for large-eddy simulations. *Phys. Fluids*, **11**(6):1596–1607.

Voke, P. and Yang, Z. (1995). Numerical study of bypass transition. *Phys. Fluids A*, **7**(9):2256–2264.